Pressure shift and broadening of the resonance line of barium atoms in liquid helium

S. I. Kanorsky, M. Arndt, R. Dziewior, A. Weis, and T. W. Hänsch
Max-Planck-Institut für Quantenoptik, Hans Kopfermann Strasse 1, D-85748 Garching, Germany
(Received 23 February 1994)

We have measured the pressure broadening and shift of the excitation and emission lines of the $6s^2\,{}^1S_0 \rightarrow 6s6p\,{}^1P_1$ transition of Ba atoms implanted in liquid and solid helium at 1.5 K. The observed spectra are quantitatively explained within the adiabatic line-broadening theory by assuming a bubble structure of the trapping sites for the Ba atoms. The evolution of the bubble shape and size in the optical excitation-deexcitation cycle is modeled theoretically.

I. INTRODUCTION

During the past decade reliable techniques for implanting atoms of practically any species in liquid He have been developed,[1–4] and extensive experimental studies of recombination and laser-induced fluorescence (LIF) spectra of atoms in a liquid-He matrix have been undertaken.[1–8] A theoretical model (the so-called bubble model[6,7]) reproduces qualitatively the character of the observed spectra, viz. a large blue shift, broadening, and asymmetry of the excitation lines and a smaller shift and broadening of the emission lines. This model, however, usually overestimates the absolute value of the excitation line shift. In the case of Ba, for example, the discrepancy is almost a factor of 9.[7] On the other hand, the same model is quite successful in describing the observed spectra of electrons trapped in liquid He at different pressures[9,10] and in solid He.[11] In Ref. 7 it was suggested that the incorporation of "better" impurity atom-He pair potentials into the model could improve the situation for atoms.

In this paper we report on the measurement of the pressure broadening and shift of the $6s^2\,{}^1S_0 - 6s6p\,{}^1P_1$ transition excitation and emission lines of atomic Ba implanted in liquid He at 1.5 K. The results obtained for pressures in the range 1–26 bar are compared with theoretical values calculated within the framework of the bubble model using adiabatic potentials for the Ba-He system.[12] In previously reported experiments[13] we have succeeded in implanting Ba atoms into a solid He matrix. The observed Ba excitation and emission spectra in that sample had similar line shapes as in liquid helium with a slightly different linewidth and line shift. No significant evidence for the effects of the crystalline structure could be found in the observed spectra, which is in contrast to the situation in heavier noble-gas matrices.

The present studies were undertaken to make a quantitative test of the model calculations and to test if, similar to electrons in condensed helium, the bubble structure of an atomic point defect is preserved in the liquid-solid phase transition.

II. EXPERIMENT

Ba atoms were implanted into liquid He contained in a copper cell with four windows for optical access. The cell was placed inside of a double-bath optical cryostat described elsewhere.[4] The lower part of the cell was immersed in liquid He at a temperature of 1.5 K. The cell had a volume of 20 cm^3, and was filled by condensing He through a 2-m-long stainless-steel capillary. The top window was a lens which focused radiation from a Nd-YAG laser onto the Ba target fixed at the bottom of the cell. As in our previous work,[4] direct ablation from a metal target with the fundamental of the pulsed Nd-YAG pulsed laser (typically 40 mJ, 9 ns) was used as the implantation method. The pressure inside the cell was measured on the room-temperature end of the capillary. A beam from a computer controlled Rh-110 dye laser traversed the cell horizontally and the laser-induced fluorescence (LIF) from the resonant $6s6p\,{}^1P_1 \rightarrow 6s^2\,{}^1S_0$ transition was collected at right angle with respect to the laser beam. The spectrum of the emitted light was analyzed with a $\frac{1}{2}$-m monochromator and a photon counting system. With an overall fluorescence detection efficiency of 4×10^{-5} the typical LIF count rate was on the order of several kHz.

Excitation spectra were taken by adjusting the monochromator to the maximum of the emission line and by scanning the laser wavelength in steps of 0.5 nm. A single measurement at every spectral point consisted in the implantation of Ba followed by LIF detection during 2 sec. The main source of noise was the poor shot-to-shot reproducibility of the Ba implantation process due to changes of the target surface condition. In order to reduce this effect we averaged over 10 excitation spectra at every pressure. Emission spectra were recorded in a similar way by fixing the dye-laser wavelength to the maximum of the excitation line and by scanning the monochromator.

Figure 1 shows the measured pressure shift of the position of the excitation line with respect to the free atomic transition

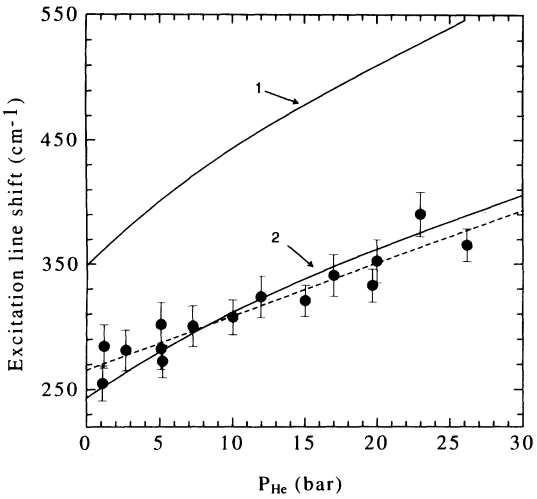

FIG. 1. Pressure shift of the excitation line of the $^1S_0 \rightarrow {}^1P_1$ transition of atomic barium in a condensed helium matrix. Black dots: experimental barycenters. Dashed line: fitted linear pressure dependence. Solid lines are the results of model calculations (see discussion in the text).

$$\Delta\varepsilon = \frac{1}{\langle\lambda\rangle} - \frac{1}{\lambda_{\text{free}}} ,$$

where $\langle\lambda\rangle$ is the barycenter of the excitation line defined by

$$\langle\lambda\rangle = \frac{\sum R_i \lambda_i}{\sum R_i} ,$$

where R_i is the LIF count rate detected with the laser wavelength λ_i. Within the experimental accuracy, the transition frequency depends linearly (indicated by the dashed line in Fig. 1) on the liquid-He pressure:

$$\Delta\varepsilon[\text{cm}^{-1}] = 265(9) + 4.3(7)p\,[\text{bar}] ;$$

with uncertainties given at the 90% confidence level. For the emission line, no significant shift was detected at saturated vapor pressure (SVP), but when increasing the pressure the line was blue shifted at a rate of 1.54(6) cm^{-1} per bar.

III. THEORETICAL MODEL

We start the discussion by recalling the main features of the theoretical model, which goes back to the earlier work of Hickman, Steets, and Lane[14] and more recent works.[6,7] The impurity atoms in liquid He reside in stable cavities with a diameter of 10 Å or larger. These cavities are formed due to a repulsion between the valence electrons of the foreign atom and the He atoms. Liquid He is described as a *continuous* medium whose density around the point defect is described by a model distribution function introduced in Ref. 15:

$$\rho(R;R_0,\alpha) = \begin{cases} 0; & R \le R_0 \\ \rho_0\{1-[1+\alpha(R-R_0)]\exp[-\alpha(R-R_0)]\}; & R \ge R_0 \end{cases} . \tag{1a}$$

From here on atomic units are used, if not explicitly specified otherwise. The density vanishes for $R \le R_0$, and asymptotically approaches the bulk density ρ_0 as $R \rightarrow \infty$. The parameter α determines the width of the transition region. For $\alpha \ge 1$ the (90−10)% interfacial width of the cavity edge is about 1.8 Å/α. The equilibrium shape of the cavity reflects the symmetry of the electronic wave function of the foreign atom, which means that a Ba atom in the $^1S_0$ ground state forms a spherical cavity. For the $^1P_1$ excited state of the Ba atom the trial function for the liquid-He density is again taken in the form (1), but the symmetry of the excited P state is taken into account by a quadrupolar angular dependence of the parameter R_0:

$$R_0'(\vartheta) = R_0\left[1+\beta\frac{3\cos^2\vartheta-1}{2}\right] , \tag{1b}$$

where ϑ is the azimuthal angle in the reference frame in which the P-state electronic wave function has the form $\Psi(\mathbf{r}) = R(\mathbf{r})Y_0^1(\vartheta,\varphi)$. In this case the equilibrium shape of the cavity is determined by the set of three parameters $\{R_0,\alpha,\beta\}$, where the parameter β determines the deviation from the spherical symmetry.

The total energy of the point defect formed by an atom in the state $|n,S,L,J\rangle$ is given by

$$E_{\text{tot}}(^{2S+1}L_J) = E_{\text{fa}}(^{2S+1}L_J) + E_{\text{int}}(^{2S+1}L_J) + E_c , \tag{2}$$

where E_{fa} is the electronic energy of the free atom, E_{int} is the energy of the interaction with the surrounding helium atoms, and E_c is the energy needed to form the cavity of a given shape. Following Hiroike *et al.*[16] the cavity contribution is commonly written as

$$E_c = 4\pi R_b^2\sigma + \frac{4}{3}\pi R_b^3 p + \frac{\hbar^2}{8M_{\text{He}}}\int\frac{(\nabla\rho)^2}{\rho}d^3R , \tag{3a}$$

where the first two terms are classical expressions for surface energy E_s and pressure work E_v for the cavity formation, and the last term represents the kinetic energy of helium atoms due to the density gradient at the edge of the cavity. The cavity radius R_b in Eq. (3a) is defined by the center of gravity of the interfacial region where the liquid-He density changes from zero to its bulk value:

$$\int_0^{R_b}\rho(r)r^2dr = \int_{R_b}^{\infty}[\rho_0-\rho(r)]r^2dr . \tag{3b}$$

In the case of a nonspherical cavity, the expressions for the surface and the volume energy take the form[17]

$$E_s = 4\pi R_b^2(1+\tfrac{4}{5}\beta^2)\sigma \ , \qquad E_v = \tfrac{4}{3}\pi R_b^3(1+\tfrac{3}{5}\beta^2)p \ . \tag{4}$$

In order to find the electronic energy of a barium atom in liquid helium one has to solve the Schrödinger equation for the two atomic valence electrons with the Hamiltonian $H_a(\mathbf{r}_1,\mathbf{r}_2)+V_{\rm int}^{\rm eff}(\rho;\mathbf{r}_1,\mathbf{r}_2)$. $H_a(\mathbf{r}_1,\mathbf{r}_2)$ is the Hamiltonian of the free atom and

$$V_{\rm int}^{\rm eff}(\rho;\mathbf{r}_1,\mathbf{r}_2)=\int d^3R\,\rho(\mathbf{R};R_0,\alpha)V_{\rm int}(\mathbf{R},\mathbf{r}_1,\mathbf{r}_2)$$

is the effective potential due to the He matrix. Here $V_{\rm int}(\mathbf{R},\mathbf{r}_1,\mathbf{r}_2)$ is the potential of the interaction with a single He atom placed at position $\mathbf{R}$ with respect to the Ba core. The foreign atom is assumed to be fixed at the cavity center $\mathbf{R}=0$. This approach involves a large amount of computation, which may not be justified considering the crude assumptions on which the model is based. Considerable simplification can be achieved, for example, by assuming that for a cavity with an equilibrium radius of approximately 6 Å the interaction of the Ba atom with a single He atom is not affected by the presence of other He atoms. The initial many-body problem is thus reduced to a two-particle problem and the total interaction energy is found as a sum over all pair interactions. The energies of these pair interactions can be directly obtained from existing theoretical adiabatic potential curves of the Ba-He system. It has been shown[6,7] that within this approach the expressions for the interaction energies of the $^1S_0$ and $^1P_1$ states are reduced to the following simple form:

$$\begin{aligned} E_{\rm int}(^1S_0) &= 4\pi\int R^2dR\,\rho(R;R_0,\alpha)V_{X^1\Sigma}(R) \ , \\ E_{\rm int}(^1P_1) &= 2\pi\int d\vartheta\sin\vartheta\int R^2dR\,\rho(R;R_0,\alpha,\beta) \\ &\quad\times[(\cos\vartheta)^2V_{B^1\Sigma}(R) \\ &\quad+(\sin\vartheta)^2V_{A^1\Pi}(R)] \ , \end{aligned} \tag{5}$$

where $V_{X^1\Sigma}(R)$, $V_{B^1\Sigma}(R)$, and $V_{A^1\Pi}(R)$ are the adiabatic potential energies of the Ba-He pair interaction shown in Fig. 2.

Equations (1)–(5) allow one to find the total energy of the point defect as a function of the cavity shape parameters $\{R_0,\alpha,\beta\}$, and the minimization of $E_{\rm tot}$ with respect to these parameters gives the equilibrium shape of the cavity $\{R_0,\alpha,\beta\}_{\rm eq}$ (in the case of the $^1S_0$ ground state $\beta\equiv 0$).

The shift of the frequency of the transition $^1S_0\rightarrow{}^1P_1$ with respect to the free atomic transition frequency is then found by assuming that the cavity shape does not change during the excitation (Franck-Condon principle):

$$\hbar\Delta\omega(R_0,\alpha)=E_{\rm int}(^1P_1)-E_{\rm int}(^1S_0) \ . \tag{6}$$

The above considerations hold also for the emission spectra; the only difference is that the emission occurs in a nonspherical cavity.

In order to calculate the spectral line profile, a line-broadening mechanism should be included in the model. In Ref. 7 an approach based on the quantization of cavity oscillations was developed. Only the lowest order (breathing) mode was considered and the shape parameters α and β were assumed to be unaffected by the cavity oscillations. The total energy of the point defect played the role of an effective potential for this oscillation, and the effective mass of the oscillator was found according to Rayleigh[17] as $M_{\rm eff}=4\pi R_b^3\rho_0$. For a cavity radius of 5 Å, $M_{\rm eff}\cong 35M_{\rm He}$. Quantization of the oscillator motion defines the probability distribution function for the cavity radius $\Psi(R)$, and the spectrum is found according to Fermi's golden rule as

$$I(\omega)\propto\left[\frac{|\Psi(R)|^2}{\partial/\partial R E_{\rm tot}(^1P_1)}\right]_{R\rightarrow R_\omega} \ , \tag{7}$$

where R_ω is the solution of the equation $\Delta\omega(R_\omega,\alpha)=\omega$.

Another approach to the line-shape calculation is to use the standard adiabatic line-broadening theory in the static limit (quasistatic line broadening theory).[18,19] This approach has been successfully used in Ref. 14 to describe the spectra of metastable excited He atoms in liquid helium. The spectrum is then given by the Fourier transform of the dipole autocorrelation function $C(\tau)$:

$$I(\omega)=\int_{-\infty}^{\infty}d\tau\,e^{i\omega\tau}C(\tau) \ . \tag{8}$$

The original formula for the autocorrelation function derived by Anderson[19] now takes the form

$$C(\tau)=\exp\left\{-\int d^3R\,\rho(\mathbf{R})\left[1-\exp\left[-\frac{i}{\hbar}\Delta V(\mathbf{R})\tau\right]\right]\right\} , \tag{9}$$

where $\Delta V(\mathbf{R})$ is the perturbation of the transition energy by a single He atom at position $\mathbf{R}$ with respect to the Ba atom and $\rho(\mathbf{R})$ is the He density distribution function (1). Equation (9) only valid if one neglects the motion of helium atoms during the correlation time $\tau_{\rm corr}$. The latter

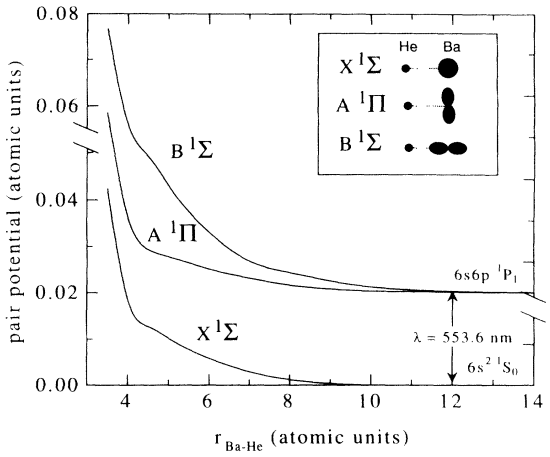

FIG. 2. Adiabatic Ba-He pair potential energies (Ref. 12) used in the present calculations.

can be estimated as the inverse of the corresponding transition line width. This gives in the case of absorption $\tau_{corr} \approx 2 \times 10^{-14}$ s and for emission $\tau_{corr} \approx 8 \times 10^{-14}$ s. The velocities of helium atoms at 1.5 K are on the order of 2.7×10^4 cm/s,[20] so that helium atoms move over a distance of only 0.15 Å during the correlation time and the condition for the applicability of the quasistatic line-broadening theory is fulfilled.

IV. DISCUSSION

The observed large difference in the shift and broadening of the excitation and emission lines originates from the difference in the size and shape of the cavities formed by Ba atom in the ground and excited states. The *shift* of the spectral line depends on the transition energy perturbation $\Delta V(\mathbf{R})$ for distances $R \geq R_b$, since the helium density drops off rapidly inside the cavity, while its *width* depends on how fast $\Delta V(\mathbf{R})$ changes in that region. As will be shown below, the excitation takes place in a smaller cavity and the excitation line is therefore more strongly perturbed by the surrounding helium. For this reason the excitation spectrum provides a more sensitive test of the model calculations and in the following discussion we will focus mainly on the latter.

A. Pressure shift of the excitation line

In the present analysis we use the numerical values of the adiabatic potential energy curves of the Ba-He pair interaction[12] shown in Fig. 2.

We have found that the method based on the quantization of the cavity breathing-mode oscillation fails to reproduce the experimentally observed excitation line shapes. The calculated values of the linewidths were smaller than the experimentally observed ones by a factor of almost 2. Conversely, the predictions of the quasistatic theory show a reasonable agreement with the experimental observations. For this reason the quasistatic theory was used to calculate the transition line shape and its barycenter.

The calculated pressure dependence of the position of the excitation line is shown in Fig. 1 as the solid line 1. The slope of the pressure dependence is well reproduced, however the offset of about 100 cm^{-1} deserves a special discussion. The quoted accuracy of the adiabatic pair potentials (10%) cannot account for this discrepancy. On one hand, it could be attributed to the intrinsic limitation of the method adopted for the calculation of the atomic energy, i.e., the reduction of the initial many-body problem to the summation of the energies of all pair interactions. On the other hand, it could also be due to the description of liquid He around the point defect as a continuous medium with the density distribution function given by the Eq. (1). For example, the minimization of the total energy of the point defect at SVP gives $R_0 = 9.3$ and $\alpha = 1.28$, for a Ba atom in the ground state. This suggests a (90−10)% interfacial width of the cavity edge of only 1.4 Å. Since the average distance between He atoms in liquid He is on the order of 3.5 Å this result is suspicious. Moreover, calculations show that the total energy of a ground state Ba atom in a spherical cavity has a shallow minimum with respect to the value of the shape parameter α. For example, for the saturated vapor pressure at 1.5 K the minimization of the total ground-state energy with respect to both shape parameters gives $E_{total}^{min} = 85$ cm^{-1} for $R_0 = 9.3$ and $\alpha = 1.3$, while fixing the value of α to 0.65 and performing the energy minimization with respect to the cavity radius R_0 only, results in $E_{total}^{min} = 100$ cm^{-1} for $R_0 = 8.84$. Although the difference of 15 cm^{-1} is larger than kT, it can hardly be considered as significant if we keep in mind that we are using the macroscopic concepts of surface tension and pressure volume work for a cavity whose diameter is comparable to the bulk interatomic separation. It is also not clear which value of the surface-tension coefficient should be used for a cavity of such a small radius. For this reason we have reversed the procedure; instead of performing a first-principles calculation of the helium density distribution and corresponding excitation spectra, we have looked for the density distribution function which gives the best description of the experimental results. The shape parameter α and the surface-tension coefficient σ were considered to be pressure independent. At every pressure point the equilibrium bubble radius was found by minimizing the total energy with respect to the parameter R_0 only. The optimum values of α and σ were found by fitting the experimental pressure dependence of the excitation line barycenter by a χ^2-minimizing procedure. The result is shown in Fig. 1 as the curve 2. The best value of normalized χ^2 of 1.2 is achieved for $\alpha = 0.6$, and $\sigma = 0.32$ erg/cm^2. The value of the surface-tension coefficient is compatible with the value 0.34 erg/cm^2 obtained in Ref. 9 from the analysis of the infrared spectra of the electron bubbles in liquid helium. The optimum value of $\alpha = 0.6$ may be interpreted as the value for which the width of the transition region is approximately equal to the interatomic separation 3.5 Å. Additional experiments with atoms of different species should be performed in order to substantiate this interpretation.

Having found a good agreement for the pressure shift of the barycenters the final test of the model calculations is done by comparing the experimental excitation line shapes with the theoretical ones calculated according to Eqs. (8) and (9), by using optimal cavity-shape parameters for each pressure. The result is shown in Fig. 3. The theory reproduces the experimentally measured widths and shifts of the excitation spectra, although it fails to exactly reproduce the observed asymmetry of the lines: the red wing of the experimental data is steeper than predicted by our calculation.

Figures 3(a)–3(c) show the Ba excitation spectra recorded in liquid helium with pressure increasing from 1 to 20 bar, while Fig. 3(d) shows the spectrum recorded in solid helium at 33 bar. There is no significant evidence for a change of the trapping site for Ba atoms when going from the liquid to the solid state of the helium matrix. The line shifts and widths recorded in solid helium are

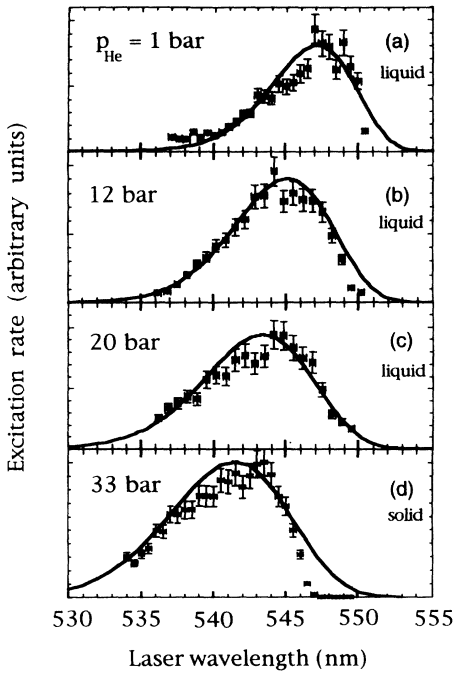

FIG. 3. Experimental and theoretical excitation line profiles of the $^1S_0 \rightarrow {}^1P_1$ transition of Ba in liquid (a)–(c) and solid (d) helium at different pressures.

still described by the bubble model developed for liquid helium with the same values of the cavity shape parameters, i.e., $\alpha = 0.6$ and $\sigma = 0.32$ erg/cm^2. However the discrepancy in the red wing of the line seems to become more pronounced for the solid helium matrix, which may partially be due to the better signal-to-noise ratio of the data points.

B. Pressure shift of the emission line

The emission spectrum of the Ba $^1S_0 \rightarrow {}^1P_1$ transition was calculated in the same way as the excitation spectrum, except for additionally allowing for a quadrupole distortion of the equilibrium bubble shape, as indicated by Eq. (1b). In order to be consistent with the results of the analysis of the excitation spectra, we set $\alpha = 0.6$ and $\sigma = 0.32$ erg/cm^2. At every pressure the value of R_0 was varied to minimize the total energy of the Ba atom in the excited $^1P_1$ state, and the value of the cavity distortion parameter β was chosen to provide the best fit to the measured pressure shift of the emission line, $(d/dp)\Delta\varepsilon_{exp} = 1.54(6)$ cm^{-1} per bar. The best agreement with the experiment is achieved for $\beta = 0.35$ with $(d/dp)\Delta\varepsilon_{theor} = 1.5$ cm^{-1} per bar. The allowance for a deviation from spherical symmetry is necessary for the explanation of the observed pressure shift rate. If we assume a spherical bubble by setting $\beta = 0$, we obtain $(d/dp)\Delta\varepsilon_{theor} = 2.4$ cm^{-1} per bar, which contradicts the experimental result.

C. Cavity evolution in the absorption-emission cycle

The results of the previous sections allow us to reconstruct the evolution of the cavity formed by the Ba atom in liquid helium in the absorption-emission cycle. The results are shown in Fig. 4. The absorption takes place in a spherical cavity of radius $R_b = 6.6$ Å [Fig. 4(a)] which is not changed during the short time of the electronic excitation [Fig. 4(b)]. The lifetime of the excited $^1P_1$ state is long enough for the bubble to settle to a new equilibrium shape:[7] $R_b = 7.6$ Å and $\beta = 0.35$. The emission thus takes place in a cavity whose shape reflects the symmetry of the excited state two-electron wave function [Figs. 4(c) and 4(d)]. For comparison we also show in Fig. 4 contour plots of squared two-electron Hartree-Fock wave functions of the free Ba atom.[12] The inner- and outermost contours represent the points in the X-Y plane where the electron density $|\Psi(x,y)|^2$ is 10^{-3} and 5×10^{-5}, respectively. The remarkable feature is that the plotted bubble shape was deduced from the analysis of the measured optical spectra, while the wave functions were obtained from independent first-principles calculations. The good agreement between the shapes provides additional support for the present model calculations.

In the recent work of Beijersbergen, Hui, and Takami[8] the change in the equilibrium bubble size due to electronic excitation was determined from the measured excitation and emission spectra of Ca, Sr, and Ba atoms implanted in liquid helium at SVP at 1.5 K. For the Ba $6s^2\,{}^1S_0 \rightarrow 6s6p\,{}^1P_1$ transition the authors found a change of the equilibrium bubble size by 2.3 Å. This result was obtained under the assumptions that the bubble has spherical shape for both the ground and the excited states, and that the equilibrium bubble radius in the

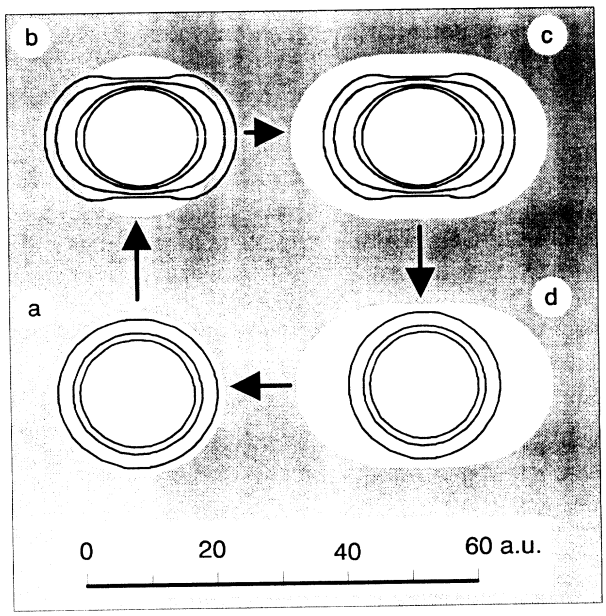

FIG. 4. Evolution of the bubble shape in the optical excitation ($a \rightarrow b$)-emission ($c \rightarrow d$) cycle, steps ($b \rightarrow c$) and ($d \rightarrow a$) are shape relaxations with the barium atom in the excited and ground state, respectively. The bubble edge is defined according to Eq. (3b) as the center of gravity of the interfacial region. The solid lines are contour plots of the two-electron-density distribution.

ground state is 6.5 Å. The latter value is in agreement with our result, while the first assumption contradicts the results of the present model calculations. The equilibrium bubble shape for the excited state shows a strong deviation from spherical symmetry as indicated in Figs. 4(c) and 4(d). The lengths of the major and minor axis of the bubble are in the ratio of 1.53:1. For this reason, we believe that the use of a single bubble size parameter by the authors of Ref. 8 is not appropriate for specifying the relaxed shape of the cavity formed by an excited Ba atom.

D. Bubble compressibility

Two effects contribute to the pressure shift of the spectral lines of foreign atom in liquid He: the increase of the helium number density (bulk compressibility) and the decrease of the equilibrium bubble radius (bubble compressibility). In the case of Ba atoms the first effect dominates, although the second is also present and can be deduced from the measured spectra. The pressure shift rate of the excitation line normalized to the liquid-helium density at SVP is

$$\left[\frac{d}{dp}\Delta\varepsilon\right]_{\text{norm}} \equiv \frac{n(p=0)}{n(p)}\frac{d}{dp}\Delta\varepsilon = 1.7(6)\text{cm}^{-1}\text{per bar}$$

(uncertainty at 90% confidence level).

For a given pressure the interaction energy in a spherical cavity calculated according to Eq. (5) is found to be well approximated by an empirical three parameter (A,B,C) function of the form

$$E_{\text{int}} = \left[\frac{A}{(R_b)^B} + C\right] n(p) , \tag{10}$$

where $n(p)$ is the bulk liquid-helium number density and the bubble radius R_b is defined according to Eq. (2a).

The pressure shift rate is then found as

$$\left[\frac{d}{dp}\Delta\varepsilon\right]_{\text{norm}} \cong -B_{^1P_1}[\Delta\varepsilon(p=0) - n(0)C_{^1P_1}]\frac{1}{R_b}\frac{\partial R_b}{\partial p} . \tag{11}$$

In Eq. (11) we have neglected the contribution to the line shift from the perturbation of the ground state, which is only about 5% of the corresponding contribution from the excited state under the equilibrium conditions. From Eq. (11) the bubble compressibility may be determined from the experimentally measured pressure shift rate and the known value of the liquid-helium bulk compressibility:

$$\kappa = -\frac{3}{R_b}\frac{\partial R_b}{\partial p} = -\frac{3}{B_{^1P_1}}\frac{[(d/dp)\Delta\varepsilon]_{\text{norm}}}{\Delta\varepsilon(p=0) - n(0)C_{^1P_1}} . \tag{12}$$

A fit of the calculated atomic energy curves gives for the Ba $^1P_1$ state $B_{^1P_1} = 6.8(1)$ and $n(0)C_{^1P_1} = -100(10)$ cm^{-1} and hence a bubble compressibility κ of $2(1)\times10^{-3}$ bar^{-1}. This value is much smaller than the compressibility of the bubble formed by a free electron in liquid helium $\kappa_e = 5.2\times10^{-2}$ bar^{-1}.[9] There are two reasons for this. First, the equilibrium bubble radius for the Ba atom is smaller than for an electron (6.5 Å instead of 17 Å), and the pressure volume work contribution to the total energy of the point defect, which is responsible for the compression of the bubble, plays only a minor role in this case. Second, due to the presence of the core electrons the wave function of the Ba valence electrons itself has smaller compressibility compared to that of an electron localized in a square-well bubble potential.

V. CONCLUSIONS

We have performed experimental studies of the pressure shift of the excitation and emission lines of the singlet $6s^2\,^1S_0 \rightarrow 6s6p\,^1P_1$ transition of Ba atoms implanted in liquid and solid helium at 1.5 K. The observed pressure shift and line broadening can be explained within the bubble model using adiabatic Ba-He pair potentials and standard adiabatic line broadening theory in the static limit. The model calculations favor the assumption that at the edge of the cavity the He density changes smoothly from zero to its bulk value over a distance which is comparable to the He interatomic separation. The performed analysis of the excitation and emission spectra enable us to reconstruct the evolution of the bubble in the optical excitation-emission cycle. No signficant evidence for the change of the trapping site for barium atom in the liquid-to-solid phase transition can be deduced from the experimental spectra, although the discrepancy between the theoretical and the experimental shape for the excitation line becomes more pronounced in solid helium.

ACKNOWLEDGMENTS

One of us (S.I.K.) thanks E. Czuchaj for providing the results of the pair potential calculations prior to publication and K. Pachucki for numerous stimulating discussions. We acknowledge excellent technical support from K. Linner and W. Simon.

[1]M. Himbert, A. Lezama, and J. Dupont-Roc, J. Phys. **46**, 2009 (1985).

[2]For a review of the works of the Heidelberg group, see, G. zu Putlitz and M. R. Beau, in *Dye Lasers: 25 Years*, edited by M. Struke (Springer, Berlin, 1992).

[3]T. Yabuzaki, A. Fujisaki, K. Sano, T. Kinoshita, and T. Takahashi, *Atomic Physics 13*, edited by H. Walther and T. W. Hänsch (North-Holland, New York, 1992).

[4]M. Arndt, S. I. Kanorsky, A. Weis, and T. W. Hänsch, Phys. Lett. A **174**, 298 (1993).

[5]A. Fujisaki, K. Sano, T. Kinoshita, Y. Takahashi, and T. Yabuzaki, Phys. Rev. Lett. **71**, 1039 (1993).

[6]A. Lezama, Ph.D. thesis, Université P. et M. Curie (Paris VI), 1981 (unpublished).

[7]H. Bauer, M. Beau, B. Friedl, C. Marchand, K. Miltner, and H. J. Reyher, Phys. Lett. A **146**, 134 (1990).
[8]J. H. M. Beijersbergen, Q. Hui, and M. Takami, Phys. Lett. A **181**, 393 (1993).
[9]C. C. Grimes and G. Adams, Phys. Rev. B **41**, 6366 (1990); **45**, 2305 (1992).
[10]A. Ya. Parshin and S. V. Pereversev, Zh. Eksp. Teor. Fiz. **101**, 126 (1992) [Sov. Phys. JETP **74**, 68 (1992)].
[11]A. I. Golov and L.P. Mezhov-Deglin, Pis'ma Zh. Eksp. Teor. Fiz. **56**, 527 (1992) [JETP Lett. **56**, 514 (1992)].
[12]E. Czuchaj (private communication).
[13]S. I. Kanorsky, M. Arndt, R. Dziewior, A. Weis, and T. W. Hänsch, Phys. Rev. B **49**, 3645 (1994).
[14]A. P. Hickman, W. Steets, and N. F. Lane, Phys. Rev. B **12**, 3705 (1975).
[15]J. Jortner, W. R. Kestner, S. A. Rice, and M. H. Cohen, J. Chem. Phys. **43**, 2614 (1965).
[16]K. Hiroike, N. R. Kestner, S. A. Rice, and J. Jortner, J. Chem. Phys. **43**, 2625 (1965).
[17]Lord Rayleigh, *Theory of Sound* (Dover, New York, 1945).
[18]S. Bloom and H. Margenau, Phys. Rev. **90**, 791 (1953).
[19]P. W. Anderson, Phys. Rev. **86**, 809 (1952).
[20]A. G. Gibbs and O. K. Harling, Phys. Rev. A **3**, 1713 (1971).

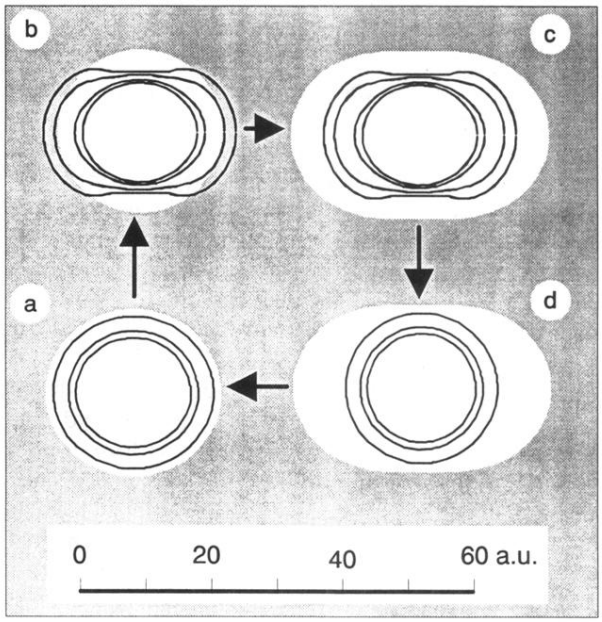

FIG. 4. Evolution of the bubble shape in the optical excitation ($a \rightarrow b$)-emission ($c \rightarrow d$) cycle, steps ($b \rightarrow c$) and ($d \rightarrow a$) are shape relaxations with the barium atom in the excited and ground state, respectively. The bubble edge is defined according to Eq. (3b) as the center of gravity of the interfacial region. The solid lines are contour plots of the two-electron-density distribution.